

DNA Enabled Chiral Gold Nanoparticle - Chromophore Hybrid Structure with Resonant Plasmon – Exciton Coupling Gives Unusual and Strong Circular Dichroism

Xiang Lan,^{†,‡} Xu Zhou,^{†,§,¶} Lauren A. McCarthy,[†] Alexander O. Govorov,^{¶,∇} Yan Liu,^{*,†,§} Stephan Link^{*,†,∥}

[†]Department of Chemistry, Rice University, 6100 Main Street, MS 60, Houston, Texas 77005, United States

[‡]Center for Molecular Design and Biomimetics at the Biodesign Institute, and [§]School of Molecular Sciences, Arizona State University, Tempe, Arizona 85287, United States

[¶]Institute of Fundamental and Frontier Sciences, University of Electronic Science and Technology of China, Chengdu 610054, China

[∇]Department of Physics and Astronomy, Ohio University, Athens, Ohio 45701, United States

[∥]Department of Electrical and Computer Engineering, Rice University, 6100 Main Street, MS 378, Houston, Texas 77005, United States

ABSTRACT: Circular dichroism (CD) from hybrid complexes of plasmonic nanostructures and chiral molecules has recently attracted significant interest. However, the hierarchical chiral self-assembly of molecules on surfaces of metal nanostructures has remained challenging. As a result, a deep understanding of plasmon-exciton coupling between surface plasmons and chiral collective molecular excitations has not been achieved. In particular, the critical impact of resonant plasmon-exciton coupling within the hybrid is unclear. Here, we employed DNA-templated strategies to control the chiral self-assembly of achiral chromophores with rationally tuned exciton transitions on gold nanosphere (AuNP) or gold nanorod (AuNR) surfaces. Unlike many previous chiral plasmonic hybrids utilizing chiral biomolecules with CD signals in the UV range, we designed structure with the chiral excitonic resonances at visible wavelengths. The constructed hybrid complexes displayed strong chiroptical activity that depends on the spectral overlap between the chiral collective molecular excitations and the plasmon resonances. We find that when spectral overlap is optimized, the molecular CD signal originating from the chiral self-assemblies of chromophores was strongly enhanced (maximum enhancement of nearly an order of magnitude) and a plasmonic CD signal was induced. Surprisingly, the sign of the molecular CD was reversed despite different self-assembly mechanisms of the Au nanoparticle-chromophore hybrids. Our results provide new insight into plasmonic CD enhancements and will inspire further studies on chiral light-matter interactions in strongly coupled plasmonic-excitonic systems.

Introduction

Controllable fabrication of nanoparticle-molecule hybrids with defined structures has profound significance in the pursuit of novel materials and functionalities.¹⁻⁷ Unprecedented collective behaviors could emerge from the engineered nanoparticle-molecule hybrids due to controlled interactions between the constituents. For

instance, through integrating metal nanoparticles and chiral molecules, molecular chirality transfer to visible wavelength plasmonic resonances⁸⁻¹⁰ was demonstrated, and has been a topic of intense research. Such chiral plasmonic hybrids exhibit great potential in ultrasensitive chiral sensing, enantioselective catalysis, and optics.¹¹⁻¹³

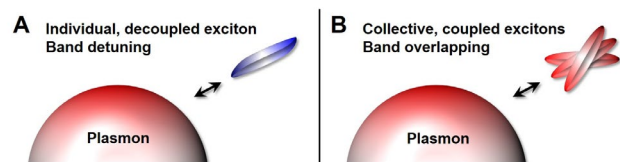
To date, a variety of plasmonic nanoparticle-chiral molecule hybrids have been created.^{9-12, 14-20} Dipole-dipole coupling⁸ or atomic surface reconfigurations²¹ are considered to be the two main chirality transfer mechanisms depending on the dimensions of the constituent nanoparticles. Previously reported nanoparticle building blocks include metal nanorods,⁹ nanocubes,²² and core-shell particles.^{14, 23} Chiral biomolecules, such as DNA,²³ peptides,²⁰ and amino acids²⁴ usually serve as the chiral molecular sources.

However, the construction of chiral plasmonic hybrid structures with controllable molecule positioning including defined separation and hierarchical self-assembly directly on nanoparticle surfaces remains a significant challenge. In previous studies, chiral molecules were often directly conjugated to nanoparticles as capping ligands^{20, 22-23, 25} or incorporated in between nanoparticles,^{9, 15, 25} without deliberate control of the molecular self-assembly. As a result, the majority of studies have been limited to weakly controlled and non-quantitative interactions between nanoparticles and non-electronically coupled isolated molecules (Scheme 1A). Specifically, coupling between nanoparticle surface plasmons and collectively coupled chiral excitons from hierarchical molecular self-assemblies is not well-understood.

Moreover, interactions between nanoparticle plasmons and molecular excitons with optimized spectral overlap leading to strong resonant coupling could greatly influence the resultant chiroptical activity. However, the majority of previous studies on hybrid complexes made from plasmonic nanostructures and chiral excitons have employed chiral molecules with absorption at ultraviolet wavelengths, far from the typical plasmon resonance of metal nanoparticles (Scheme 1A).^{13, 20, 22, 24} To explore the critical role of

resonant coupling, rational design and self-assembly of chiral plasmonic hybrids with tunable molecular excitons and plasmons are required.

Herein, we report a systematic study of the critical influence of spectral overlap and resonant coupling in chiral molecule-nanoparticle hybrids via rational engineering of molecular self-assembly on metal nanoparticle surfaces (Scheme 1B). DNA nanotechnology has proven to be a powerful tool to rationally design and precisely control the self-organization of nanoparticles and molecules.^{4, 26-40} Through DNA-templated strategies, we constructed three different types of chiral plasmonic Au nanoparticle-chromophore hybrid structures. These hybrids include a complex of AuNRs and cyanine dye K21 J-type aggregates on DNA duplexes, and two complexes of AuNPs and cyanine dye (Cy3 or Cy5) dimers constructed in the middle of DNA duplexes. The chromophores are all individually achiral but display collectively coupled chiral excitons when they self-assemble with the aid of the DNA duplex templates. We find that the chirality of the Au nanoparticle-chromophore hybrids has contributions from both molecular CD of the chiral self-assemblies of chromophores and induced plasmonic CD by the chiral self-assemblies. Surprisingly, the sign of the molecular CD is reversed with an enhanced magnitude compared to the DNA templates and chromophores only. The signal intensities of both the molecular CD and plasmonic CD depends on the spectral overlap between the surface plasmons and the collective chiral excitons of the chromophores. All of these features specific to the hybrids highlight the critical impact of resonant coupling between the Au nanostructures and the chiral self-assemblies of chromophores.



Scheme 1. Key differences between previously reported chiral molecule-plasmonic hybrids (A) and the hybrids in this work (B). (A) Shows an individual chiral molecule, while (B) shows a chiral assembly of achiral molecules in proximity to the metal nanoparticle surface. Differing exciton absorption wavelengths of the molecules are shown in blue and red, indicating poor and good spectral overlap with the surface plasmon, respectively.

Results and Discussion

By taking advantage of the strong binding of K21 cyanine dyes to double-stranded DNA (dsDNA),⁴¹ we assembled K21 aggregates on dsDNA-functionalized AuNRs (Figure 1A). The dsDNA strands (17 bp) were pre-hybridized on AuNRs (~10 nm × 44 nm), and then K21 was added to bind to the dsDNA through electrostatic attractions to the negatively charged DNA and hydrophobic interactions with the bases. After K21 binding to the dsDNA, a new extinction band with a maximum at 460 nm appeared in the spectrum (Figure 1B). This red-shifted resonance relative to K21 monomer indicates the formation of J-type aggregates of K21 on dsDNA with an end-to-end configuration.⁴² The AuNRs have two separate plasmon resonances, a transverse mode centered at 510 nm and a longitudinal mode centered at 725 nm (Figure 1B). The collective exciton of the K21 aggregates overlaps with the tail of the AuNR transverse plasmon, but is far away from the longitudinal plasmon. These spectral features enable us to investigate the influence of relative spectral positions between plasmons and collective excitons on the chiroptical response of the AuNR-K21 hybrid.

We found that the chiroptical response is highly impacted by the coupling between the collective excitations of the K21 aggregates and the AuNR transverse plasmon mode. As shown in Figure 1C, the dsDNA templated K21 aggregates alone displayed a sharp

peak-dip CD lineshape (red), compared with the featureless CD spectrum of free K21 (blue). The zero crossing point of the CD spectrum at 460 nm is coincident with the maximum absorption wavelength of K21 aggregates on dsDNA (Figure 1B). When K21 aggregates were assembled on the DNA duplexes and aligned on the AuNR surface, the original molecular CD dip was reversed in sign to produce a sharp peak at 465 nm with an order of magnitude enhanced intensity (Figure 1D). The intensity enhancement can be seen directly by comparing the magnitudes of the CD spectra in Figure 1C and 1D, which are expressed in units of molar ellipticity. In addition a new broad CD peak arose at ~510 nm, coincident with the AuNR transverse plasmon mode. The observations of sign reversal for the molecular CD and the appearance of plasmonic CD were reproducible with different K21 concentrations (Figure S1). The AuNR-dsDNA complexes without K21 displayed a featureless CD spectrum (Figure 1D). Also, no CD signal was detected from AuNR-K21 hybrids at the longitudinal plasmon mode around 725 nm due to significantly reduced spectral overlap between the longitudinal plasmon mode and the collective excitons of the K21 aggregates. This result indicates that spectral overlap leading to resonant coupling plays a critical role in the observed chirality of the AuNR-K21 hybrid.

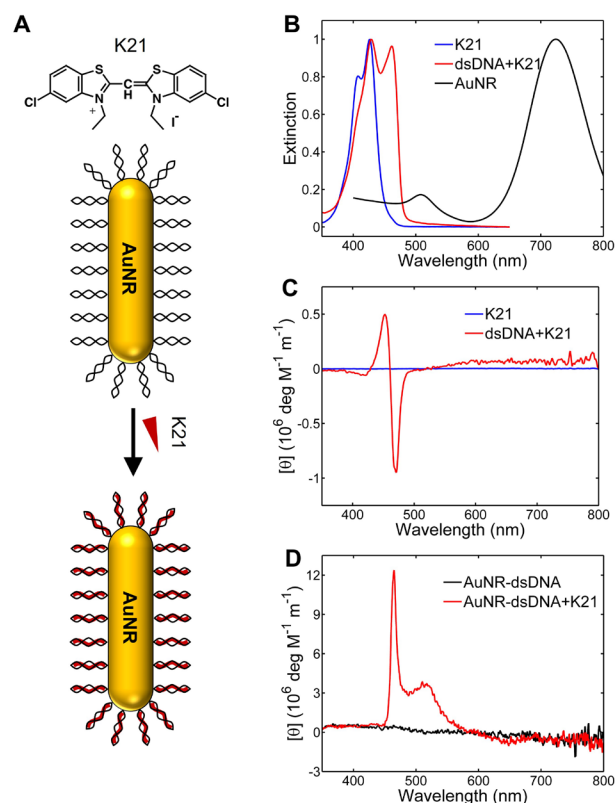


Figure 1. A) Schematic of the self-assembly of the hybrid complex of AuNR-K21 aggregates, templated by dsDNA conjugated on the AuNR surface. B) Normalized extinction spectra of aqueous solutions of K21 before (blue) and after (red) binding to dsDNA and of AuNRs alone (black). C) CD spectra of K21 before and after binding to dsDNA. D) CD spectra of AuNRs conjugated with dsDNA before and after K21 self-assembly on the DNA templates. The molar ratio of K21 to dsDNA on the AuNR surface was set to 160 in the reaction. All the CD spectra in panels C and D were normalized to the dsDNA concentration to obtain the molar ellipticity, except for the K21 only sample, which was normalized by the K21 concentration. The number of ssDNA per AuNR before DNA hybridizations to form dsDNA was estimated to be ~125 using Mirkin's model.⁴³ All the ssDNAs conjugated to the AuNR surface were assumed to hybridize with their complementary strands to produce dsDNAs when calculating the molar ellipticity of the hybrid.

Therefore, the molar ellipticity of the AuNR-K21 hybrid normalized by the dsDNA concentration is likely even higher than the values shown in panel D.

We did not observe CD at the longitudinal plasmon mode of the AuNRs, despite the potential existence of minor AuNR aggregation that could improve the molecular chirality transfer to the longitudinal mode through local electric field enhancement.⁹ The extinction spectra of AuNRs showed a red-shift of 10-30 nm after K21 binding for both plasmon modes (Figure S2). This spectral shift likely results from an increased refractive index of the surroundings⁴⁴ and potentially the occurrence of AuNR aggregation due to electrostatic interactions between K21 and dsDNA-capped AuNRs. The lack of observable CD at the longitudinal plasmon resonance, however, indicates that only minor AuNR aggregation could have occurred on the measurement timescale. Otherwise, the strong electromagnetic hot spots generated in the nanoparticle aggregate gaps should have enabled a plasmonic CD signal at the longitudinal mode induced by the K21 assemblies despite the poor spectral overlap.¹³

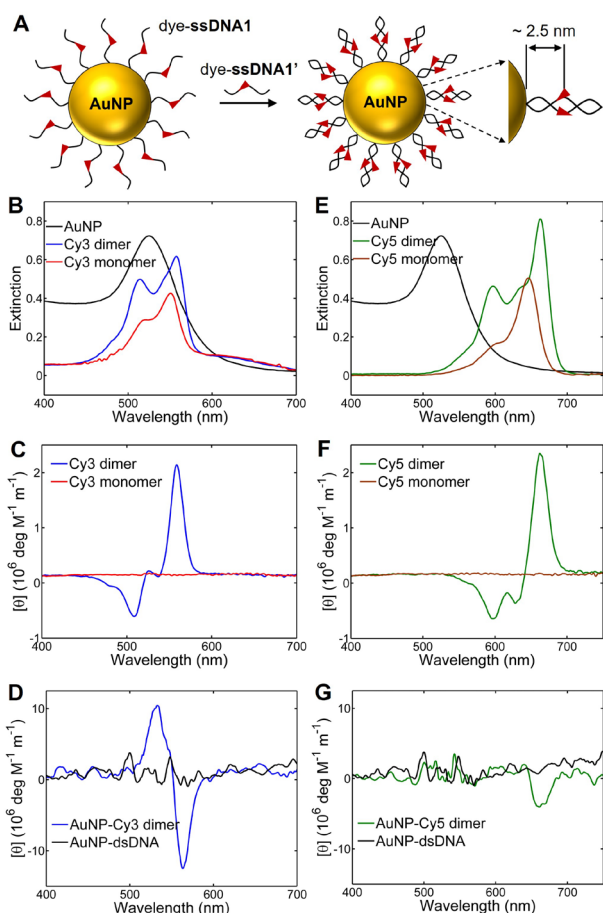


Figure 2. A) Schematic of the dsDNA mediated self-assembly of the AuNP-dye dimer hybrids. Note that any ssDNAs with only a single dye that may remain unhybridized on the AuNP surface are not shown, because single dyes conjugated to ssDNAs are not observed to contribute to the CD of the hybrid (Figure S3). Experimentally measured extinction (B and E) and CD spectra (C, D, F and G) demonstrate the importance of spectral overlap on the CD intensity and sign for the AuNP-dye dimer hybrids. Cy3 (B-D) and Cy5 (E-G) were used for the sample preparation. In all panels, dye monomer refers to a single dye conjugated to ssDNA, while dye dimer denotes two coupled dyes organized by dsDNA. All CD spectra were normalized to the DNA concentrations (ssDNA or dsDNA) to obtain the molar ellipticity for direct quantitative comparison.

To achieve more quantitative insight, we utilized a dsDNA hybridization strategy to engineer AuNP-cyanine dye dimer hybrids with more precise control over the number of attached dye molecules and the AuNP-dye distances. Cy3 or Cy5 dyes with distinct electronic transition wavelengths were rationally selected to obtain a large spectral overlap for Cy3 or a large spectral separation for Cy5 with respect to the plasmon resonance for 30 nm AuNPs centered at 525 nm.

A schematic of the self-assembly for the AuNP-dye dimer hybrid is shown in Figure 2A. Thiolated single-stranded DNA (ssDNA1, 16 nt) with a single dye (Cy3 or Cy5) modified in the middle of the sugar-phosphate backbone was first attached to the AuNP surface through Au-S linkage. This step was followed by the addition of a fully complementary DNA (ssDNA1', 16 nt), also with a single dye of the same type labeled in the middle of the backbone. After DNA hybridization with 8 bp flanking each side of the pair of dyes in the middle, a layer of chiral dye dimers was organized around the AuNP. The layer of the dye-dimers was separated from the AuNP surface with a distance of approximately 2.5 nm (8bp, 0.335 nm/bp) (Figure 2A). Note that one must keep two dsDNA fragments (i.e. 8bp here) flanking each side of the dye dimer in order to ensure the stability of the dye dimer. After we estimated the thermal stability of the dsDNA fragment based on its length, we cautiously chose the 8bp length of the dsDNA fragments, because this length is close to the minimum value that can keep the fragment stable under our mild experimental condition.

Molecular dynamics simulations have predicted different conformations of dye dimers associated with the neighboring nucleotides in the DNA duplex template.⁴⁵⁻⁴⁶ Here the formation of the dye dimers caused a clear red-shift of the lowest electronic transition compared to dye monomer from 550 nm to 560 nm for Cy3 and from 645 nm to 660 nm for Cy5 (Figures 2B and 2E).⁴⁷ This red-shift is indicative of anti-symmetric dipole-dipole coupling similar to that in a J-type aggregate.⁴⁵⁻⁴⁶ The exciton transition for the Cy3 dimer located around 560 nm has significant spectral overlap with the AuNP plasmon (Figure 2B). In contrast, the corresponding transition for the Cy5 dimer at about 660 nm is shifted away from the AuNP plasmon (Figure 2E). It is noteworthy that the CD spectra of the Cy3 and Cy5 dimers alone in the dsDNA template have similar CD lineshapes with a strong peak at the 0-0 transition and a relatively weak dip at the 0-1 transition (Figures 2C and 2F). Both dye dimers therefore have similar collective excitations and dipole-dipole interactions among the constituent monomers. As expected, both the achiral Cy3 and Cy5 monomers conjugated with ssDNA without the AuNP showed no CD signals in the visible region (Figures 2C and 2F).

When dye dimers were assembled on the AuNP surfaces, the CD of the hybrid (Figures 2D and 2G) drastically changed from that without AuNPs (Figures 2C and 2F). The CD spectra of AuNP-dye dimer hybrids and dsDNA-dye dimers were compared after normalization to the dsDNA concentration (i.e. dye dimer concentration). The number of dye dimers per AuNP was estimated to be ~ 70 by using gel electrophoresis and band intensity analysis (Figures S4 and S5). For the AuNP-Cy3 dimer hybrid, a plasmonic CD peak at 530 nm close to the AuNP plasmon resonance at 525 nm appeared, accompanied by a sign reversal of the molecular CD around 560 nm. In addition, the intensity of the molecular CD arising from the collective transitions in the Cy3 dimer was enhanced by a factor of ~ 6 through coupling to the plasmon resonance in the AuNP-dye dimer hybrid, compared to the dye dimer only (Figures 2C and 2D). When Cy5 was employed in forming the dye dimer on the AuNP surfaces, only a weak molecular CD at 660 nm was observed with an enhancement factor of ~ 1.5 (Figures 2F and 2G). While the molecular CD similarly showed a sign reversal, no plasmonic CD could be detected at 525 nm.

DNA duplex-decorated AuNPs without the dye dimers showed no detectable CD signals in the same spectral range (Figures 2D and 2G), indicating that DNA duplexes minimally contribute to the CD signals of the AuNP-dye dimer hybrids, compared to the chiral dye dimers. We also investigated the CD from AuNP aggregates that might have existed at small quantities and could have contributed to CD through strong enhancement of molecular chirality transfer from the DNA and dye dimers in electromagnetic hot spots (Figure S6). We deliberately hybridized two batches of AuNPs decorated with complementary ssDNA labeled with a single Cy3 and produced random AuNP aggregates with Cy3 dimers in between neighboring AuNPs. However, no CD signal was detected. We prepared dilute AuNP aggregates as a control, because the sharp gel bands of the AuNP-Cy3 dimer in Figures S4 and S5 indicate scarce or no existing AuNP aggregation. On the other hand, there is likely only very few Cy3 dimers in the nanoparticle gap due to the steric hindrance between AuNPs, which could also be an explanation for no observation of a CD signal. Overall, no observation of CD signal from AuNP aggregates indicates that the chiral dye dimers on single AuNPs was the basis for the observed CD spectra.

The significantly different chiroptical activities induced by the Cy3 and Cy5 chiral dimers are undoubtedly a result of their distinct couplings with the AuNP plasmon. With a larger spectral overlap between the chiral collective exciton transitions and the AuNP plasmon in the case of Cy3, resonant-like strong coupling occurred and caused a larger CD enhancement for both molecular and plasmonic CD, accompanied by a sign reversal of the molecular CD. These observations are consistent with those observed in the AuNR-K21 aggregates, demonstrating the generality of our findings across both systems studied here.

Previous theoretical reports have shown that molecular CD mildly changes when interacting with surface plasmons in a non-resonant hybrid.⁸ Such relatively-weak, non-resonant effects were indeed observed in several experimental studies using chiral biomolecules, such as DNAs and peptides^{20, 48}. In these non-resonant structures, the near-field Coulomb interaction between the molecular and plasmonic components typically creates the so-called plasmon-induced CD, which appears at the plasmon resonance of the non-chiral nanoparticle.^{8, 13, 20, 48} In contrast, the molecular CD is expected to be more complex in a resonant hybrid. In this case, molecular CD lines could be strongly enhanced or suppressed depending on the orientation of individual molecular dipoles relative to the nanoparticle surface.^{8, 13} In addition, strong exciton-plasmon Fano interferences or hybridization could impact the spectral shape of the plasmon-induced CD.⁸ So far, mostly the non-resonant regime of plasmon-induced CD has been modeled^{8, 13} and we cannot apply such non-resonant theory directly to our case. However, one of the central results of the theory of Coulomb-assisted molecular-plasmon CD can be utilized for our case. This result tells us that the plasmonic enhancement of molecular CD signals is inversely proportional to the spectral distance between the molecular line and the plasmonic peak, $\lambda_{\text{plasmon}} - \lambda_{\text{exciton}}$. We observe this behavior in Figure 2. For the resonant case in Figure 2d, the enhancement of the molecular CD is 6-fold, whereas the non-resonant case in Figure 2g exhibits a smaller enhancement factor (<2).

In previous theoretical studies of nanoparticles interacting with a single chiral molecule, the calculated internal molecular absorption is enhanced when the molecular exciton and the nanoparticle plasmon are resonant.⁸ This absorption enhancement could be an explanation for the molecular CD enhancement observed here. Regarding the sign reversal of the molecular CD, we hypothesize that the chiral collective excitons of the chromophores are modulated by the nanoparticle plasmon due to the strong near-field coupling between them. This collective interaction correlated with the local fields on the nanoparticle surface is distinct from the exciton-exciton coupling in the uniform light field without the nanoparticle. For

example, theoretical studies have demonstrated that the CD lineshape of Cy3 dimers without the AuNP is associated with the symmetric and anti-symmetric coupling between the excitons.⁴⁵ One would expect that the electric polarizability of the dye could be greatly influenced through the near-field coupling with the nanoparticle when they are in close proximity. This near-field coupling will further impact the symmetric and anti-symmetric coupling between the molecular excitons and potentially modify the orientation of the collective dipoles with respect to the nanoparticle plasmon, which could drastically change the molecular CD lineshape.⁸ We also note that the mechanisms of interaction between a chiral molecule and a plasmonic nanoparticle can be of two types: (1) the Coulomb interaction between molecular and plasmonic dipoles and (2) short-range orbital (contact) interaction between a chiral molecule and the surface of a nanoparticle. Clearly, more theoretical studies are needed to understand this class of chiroptical effects appearing in the chiral plasmonic hybrids introduced here.

Conclusions

To summarize, we rationally constructed three different types of chiral Au nanoparticle-chromophore hybrid complexes using DNA templated strategies, featuring tunable chiral collective molecular excitations relative to the plasmon modes. We found that spectral overlap between plasmons and the collectively coupled chiral excitons lead to enhanced molecular CD with a maximum enhancement factor close to 10 and induction of plasmonic CD. In contrast, collective molecular excitons without significant spectral overlap with the plasmon resonances showed rather weak enhancement of molecular CD. Similarly, plasmon modes without significant spectral overlap with the collective molecular excitons displayed no distinguishable plasmonic CD. In addition, we found that the sign of molecular CD was reversed for all different Au nanoparticle-chromophore hybrids compared to the chromophore-DNA only structures, despite the different self-assembly strategies employed here. We envision that this study will inspire the rational design and construction of nanoparticle-molecule hybrid architectures with increased hierarchy, complexity, and chiral coupling, utilizing the power of DNA nanotechnology. Furthermore, our findings provide new insights into chiral molecule-nanoparticle interactions, and inspire new possibilities for strongly coupled chiral systems, which have significant potential in achieving chiral molecule sensing on the single molecule level.

ASSOCIATED CONTENT

Supporting Information

The Supporting Information is available free of charge on the ACS Publications website. Materials and methods, DNA sequences, and supplementary figures.

AUTHOR INFORMATION

#These authors contributed equally

Corresponding Author

Yan_Liu@asu.edu
slink@rice.edu

Notes

The authors declare no competing financial interests.

ACKNOWLEDGMENT

This work is funded by the Robert A. Welch Foundation (C-1664 to S.L.) and the National Science Foundation (CHE1507745 and CHE1903980 to S.L.). L.A.M. acknowledges the support by the

National Science Foundation Graduate Research Fellowship Program (1450681). Y.L. and X.Z. acknowledge the support from the U.S. Department of Energy (DE-SC0016353). The authors thank Prof. David Whitten who generously provided the sample of K21 dye used in this study. The authors also thank Mr. Bo Jiang and Dr. Ali Rafiei-Miandashti for their help with the experiments.

REFERENCES

- (1) Choueiri, R. M.; Galati, E.; Therien-Aubin, H.; Klinkova, A.; Larin, E. M.; Querejeta-Fernandez, A.; Han, L. L.; Xin, H. L.; Gang, O.; Zhulina, E. B.; Rubinstein, M.; Kumacheva, E. Surface patterning of nanoparticles with polymer patches. *Nature* **2016**, *538*, 79-83.
- (2) Pastoriza-Santos, I.; Kinnear, C.; Perez-Juste, J.; Mulvaney, P.; Liz-Marzan, L. M. Plasmonic polymer nanocomposites. *Nat. Rev. Mater.* **2018**, *3*, 375-391.
- (3) Liu, K.; Nie, Z. H.; Zhao, N. N.; Li, W.; Rubinstein, M.; Kumacheva, E. Step-Growth Polymerization of Inorganic Nanoparticles. *Science* **2010**, *329*, 197-200.
- (4) Jones, M. R.; Seeman, N. C.; Mirkin, C. A. Programmable materials and the nature of the DNA bond. *Science* **2015**, *347*, 1260901.
- (5) Liu, X. G.; Zhang, F.; Jing, X. X.; Pan, M. C.; Liu, P.; Li, W.; Zhu, B. W.; Li, J.; Chen, H.; Wang, L. H.; Lin, J. P.; Liu, Y.; Zhao, D. Y.; Yan, H.; Fan, C. H. Complex silica composite nanomaterials templated with DNA origami. *Nature* **2018**, *559*, 593-598.
- (6) Yeom, J.; Santos, U. S.; Chekini, M.; Cha, M.; de Moura, A. F.; Kotov, N. A. Chiro-magnetic nanoparticles and gels. *Science* **2018**, *359*, 309-314.
- (7) Chen, C. L.; Zhang, P. J.; Rosi, N. L. A new peptide-based method for the design and synthesis of nanoparticle superstructures: Construction of highly ordered gold nanoparticle double helices. *J. Am. Chem. Soc.* **2008**, *130*, 13555-13557.
- (8) Govorov, A. O.; Fan, Z. Y.; Hernandez, P.; Slocik, J. M.; Naik, R. R. Theory of Circular Dichroism of Nanomaterials Comprising Chiral Molecules and Nanocrystals: Plasmon Enhancement, Dipole Interactions, and Dielectric Effects. *Nano Lett.* **2010**, *10*, 1374-1382.
- (9) Han, B.; Zhu, Z. N.; Li, Z. T.; Zhang, W.; Tang, Z. Y. Conformation Modulated Optical Activity Enhancement in Chiral Cysteine and Au Nanorod Assemblies. *J. Am. Chem. Soc.* **2014**, *136*, 16104-16107.
- (10) Li, Z. T.; Zhu, Z. N.; Liu, W. J.; Zhou, Y. L.; Han, B.; Gao, Y.; Tang, Z. Y. Reversible Plasmonic Circular Dichroism of Au Nanorod and DNA Assemblies. *J. Am. Chem. Soc.* **2012**, *134*, 3322-3325.
- (11) Ma, W.; Xu, L. G.; de Moura, A. F.; Wu, X. L.; Kuang, H.; Xu, C. L.; Kotov, N. A. Chiral Inorganic Nanostructures. *Chem. Rev.* **2017**, *117*, 8041-8093.
- (12) Hendry, E.; Carpy, T.; Johnston, J.; Popland, M.; Mikhaylovskiy, R. V.; Laphorn, A. J.; Kelly, S. M.; Barron, L. D.; Gadegaard, N.; Kadodwala, M. Ultrasensitive detection and characterization of biomolecules using superchiral fields. *Nat. Nanotechnol.* **2010**, *5*, 783-787.
- (13) Besteiro, L. V.; Zhang, H.; Plain, J.; Markovich, G.; Wang, Z. M.; Govorov, A. O. Aluminum Nanoparticles with Hot Spots for Plasmon-Induced Circular Dichroism of Chiral Molecules in the UV Spectral Interval. *Adv. Opt. Mater.* **2017**, *5*, 1700069.
- (14) Bao, Z. Y.; Zhang, W.; Zhang, Y. L.; He, J. J.; Dai, J. Y.; Yeung, C. T.; Law, G. L.; Lei, D. Y. Interband Absorption Enhanced Optical Activity in Discrete Au@Ag Core-Shell Nanocuboids: Probing Extended Helical Conformation of Chemisorbed Cysteine Molecules. *Angew. Chem. Int. Edit.* **2017**, *56*, 1283-1288.
- (15) Dominguez-Medina, S.; Kiskey, L.; Tauzin, L. J.; Hoggard, A.; Shuang, B.; Indrasekara, A. S. D. S.; Chen, S. S.; Wang, L. Y.; Derry, P. J.; Liopo, A.; Zubarev, E. R.; Landes, C. F.; Link, S. Adsorption and Unfolding of a Single Protein Triggers Nanoparticle Aggregation. *ACS Nano* **2016**, *10*, 2103-2112.
- (16) George, J.; Thomas, K. G. Surface Plasmon Coupled Circular Dichroism of Au Nanoparticles on Peptide Nanotubes. *J. Am. Chem. Soc.* **2010**, *132*, 2502-2503.
- (17) Knoppe, S.; Wong, O. A.; Malola, S.; Hakkinen, H.; Burgi, T.; Verbiest, T.; Ackerson, C. J. Chiral Phase Transfer and Enantioenrichment of Thiolate-Protected Au-102 Clusters. *J. Am. Chem. Soc.* **2014**, *136*, 4129-4132.
- (18) Maoz, B. M.; Chaikin, Y.; Tesler, A. B.; Bar Elli, O.; Fan, Z. Y.; Govorov, A. O.; Markovich, G. Amplification of Chiroptical Activity of Chiral Biomolecules by Surface Plasmons. *Nano Lett.* **2013**, *13*, 1203-1209.
- (19) Maoz, B. M.; van der Weegen, R.; Fan, Z. Y.; Govorov, A. O.; Ellestad, G.; Berova, N.; Meijer, E. W.; Markovich, G. Plasmonic Chiroptical Response of Silver Nanoparticles Interacting with Chiral Supramolecular Assemblies. *J. Am. Chem. Soc.* **2012**, *134*, 17807-17813.
- (20) Slocik, J. M.; Govorov, A. O.; Naik, R. R. Plasmonic Circular Dichroism of Peptide-Functionalized Gold Nanoparticles. *Nano Lett.* **2011**, *11*, 701-705.
- (21) Gautier, C.; Burgi, T. Chiral inversion of gold nanoparticles. *J. Am. Chem. Soc.* **2008**, *130*, 7077-7084.
- (22) Lu, F.; Tian, Y.; Liu, M.; Su, D.; Zhang, H.; Govorov, A. O.; Gang, O. Discrete Nanocubes as Plasmonic Reporters of Molecular Chirality. *Nano Lett.* **2013**, *13*, 3145-3151.
- (23) Wu, X. L.; Xu, L. G.; Ma, W.; Liu, L. Q.; Kuang, H.; Yan, W. J.; Wang, L. B.; Xu, C. L. Gold Core-DNA-Silver Shell Nanoparticles with Intense Plasmonic Chiroptical Activities. *Adv. Funct. Mater.* **2015**, *25*, 850-854.
- (24) Zhu, Z. N.; Liu, W. J.; Li, Z. T.; Han, B.; Zhou, Y. L.; Gao, Y.; Tang, Z. Y. Manipulation of Collective Optical Activity in One-Dimensional Plasmonic Assembly. *ACS Nano* **2012**, *6*, 2326-2332.
- (25) Lan, X.; Wang, Q. B. Optically Active AuNR@Ag Core-Shell Nanoparticles and Hierarchical Assembly via DNA-Mediated Surface Chemistry. *ACS Appl. Mater. Interfaces* **2016**, *8*, 34598-34602.
- (26) Sharma, J.; Chhabra, R.; Cheng, A.; Brownell, J.; Liu, Y.; Yan, H. Control of Self-Assembly of DNA Tubules Through Integration of Gold Nanoparticles. *Science* **2009**, *323*, 112-116.
- (27) Kuzyk, A.; Schreiber, R.; Fan, Z. Y.; Pardatscher, G.; Roller, E. M.; Hoge, A.; Simmel, F. C.; Govorov, A. O.; Liedl, T. DNA-based self-assembly of chiral plasmonic nanostructures with tailored optical response. *Nature* **2012**, *483*, 311-314.
- (28) Kuzyk, A.; Schreiber, R.; Zhang, H.; Govorov, A. O.; Liedl, T.; Liu, N. Reconfigurable 3D plasmonic metamolecules. *Nat. Mater.* **2014**, *13*, 862-866.
- (29) Lan, X.; Su, Z. M.; Zhou, Y. D.; Meyer, T.; Ke, Y. G.; Wang, Q. B.; Chiu, W.; Liu, N.; Zou, S. L.; Yan, H.; Liu, Y. Programmable Supra-Assembly of a DNA Surface Adapter for Tunable Chiral Directional Self-Assembly of Gold Nanorods. *Angew. Chem. Int. Edit.* **2017**, *56*, 14632-14636.
- (30) Lan, X.; Lu, X. X.; Shen, C. Q.; Ke, Y. G.; Ni, W. H.; Wang, Q. B. Au Nanorod Helical Superstructures with Designed Chirality. *J. Am. Chem. Soc.* **2015**, *137*, 457-462.
- (31) Wang, P. F.; Gaitanos, S.; Lee, S.; Bathe, M.; Shih, W. M.; Ke, Y. G. Programming Self-Assembly of DNA Origami Honeycomb Two-Dimensional Lattices and Plasmonic Metamaterials. *J. Am. Chem. Soc.* **2016**, *138*, 7733-7740.
- (32) Voigt, N. V.; Topping, T.; Rotaru, A.; Jacobsen, M. F.; Ravnsbaek, J. B.; Subramani, R.; Mamdouh, W.; Kjems, J.; Mokhir, A.; Besenbacher, F.; Gothelf, K. V. Single-molecule chemical reactions on DNA origami. *Nat. Nanotechnol.* **2010**, *5*, 200-203.
- (33) Macfarlane, R. J.; Lee, B.; Jones, M. R.; Harris, N.; Schatz, G. C.; Mirkin, C. A. Nanoparticle Superlattice Engineering with DNA. *Science* **2011**, *334*, 204-208.
- (34) Aldaye, F. A.; Palmer, A. L.; Sleiman, H. F. Assembling materials with DNA as the guide. *Science* **2008**, *321*, 1795-1799.
- (35) Trinh, T.; Liao, C. Y.; Toader, V.; Barlog, M.; Bazzi, H. S.; Li, J. N.; Sleiman, H. F. DNA-imprinted polymer nanoparticles with monodispersity and prescribed DNA-strand patterns. *Nat. Chem.* **2018**, *10*, 184-192.
- (36) Alivisatos, A. P.; Johnsson, K. P.; Peng, X. G.; Wilson, T. E.; Loweth, C. J.; Bruchez, M. P.; Schultz, P. G. Organization of 'nanocrystal molecules' using DNA. *Nature* **1996**, *382*, 609-611.
- (37) Jiang, Q.; Xu, X. H.; Yin, P. A.; Ma, K.; Zhen, Y. G.; Duan, P. F.; Peng, Q.; Chen, W. Q.; Ding, B. Q. Circularly Polarized Luminescence of Achiral Cyanine Molecules Assembled on DNA Templates. *J. Am. Chem. Soc.* **2019**, *141*, 9490-9494.
- (38) Shen, C.; Lan, X.; Zhu, C.; Zhang, W.; Wang, L.; Wang, Q. Spiral Patterning of Au Nanoparticles on Au Nanorod Surface to Form Chiral AuNR@AuNP Helical Superstructures Templated by DNA Origami. *Adv. Mater.* **2017**, *29*, 1606533.
- (39) Shen, C.; Lan, X.; Lu, X.; Ni, W.; Wang, Q. Tuning the structural asymmetries of three-dimensional gold nanorod assemblies. *Chem. Commun.* **2015**, *51*, 13627-13629.
- (40) Chen, Z.; Lan, X.; Chiu, Y. C.; Lu, X.; Ni, W.; Gao, H.; Wang, Q. Strong Chiroptical Activities in Gold Nanorod Dimers Assembled Using DNA Origami Templates. *ACS Photonics* **2015**, *2*, 392-397.
- (41) Zhou, X.; Mandal, S.; Jiang, S. X.; Lin, S.; Yang, J. Z.; Liu, Y.; Whitten, D. G.; Woodbury, N. W.; Yan, H. Efficient Long-Range, Directional Energy Transfer through DNA-Templated Dye Aggregates. *J. Am. Chem. Soc.* **2019**, *141*, 8473-8481.
- (42) Wang, M. M.; Silva, G. L.; Armitage, B. A. DNA-templated formation of a helical cyanine dye J-aggregate. *J. Am. Chem. Soc.* **2000**, *122*, 9977-9986.

(43) Hill, H. D.; Millstone, J. E.; Banholzer, M. J.; Mirkin, C. A. The Role Radius of Curvature Plays in Thiolated Oligonucleotide Loading on Gold Nanoparticles. *ACS Nano*. **2009**, *3*, 418-424.

(44) Lee, K. S.; El-Sayed, M. A. Dependence of the enhanced optical scattering efficiency relative to that of absorption for gold metal nanorods on aspect ratio, size, end-cap shape, and medium refractive index. *J. Phys. Chem. B*. **2005**, *109*, 20331-20338.

(45) Kringle, L.; Sawaya, N. P. D.; Widom, J.; Adams, C.; Raymer, M. G.; Aspuru-Guzik, A.; Marcus, A. H. Temperature-dependent conformations of exciton-coupled Cy3 dimers in double-stranded DNA. *J. Chem. Phys.* **2018**, *148*, 085101.

(46) Cunningham, P. D.; Kim, Y. C.; Diaz, S. A.; Buckhout-White, S.; Mathur, D.; Medintz, I. L.; Melinger, J. S. Optical Properties of

Vibronically Coupled Cy3 Dimers on DNA Scaffolds. *J. Phys. Chem. B*. **2018**, *122*, 5020-5029.

(47) Mastroph, H.; Reiner, K.; Mistol, J.; Ernst, S.; Keil, D.; Hennig, L. Relationship between the Molecular Structure of Cyanine Dyes and the Vibrational Fine Structure of their Electronic Absorption Spectra. *Chem. Phys. Chem.* **2009**, *10*, 835-840.

(48) Shen, X. B.; Zhan, P. F.; Kuzyk, A.; Liu, Q.; Asenjo-Garcia, A.; Zhang, H.; de Abajo, F. J. G.; Govorov, A.; Ding, B. Q.; Liu, N. 3D plasmonic chiral colloids. *Nanoscale*. **2014**, *6*, 2077-2081.

